

Article

Sprinkler Irrigation on Sloping Land: Distribution Characteristics of Droplet Impact Angle and Shear Stress

Xin Hui ^{1,2}, Yifei Chen ¹, Muhammad Rizwan Shoukat ² , Huimin Yang ^{1,*} and Yudong Zheng ^{2,*}

¹ Institute of Mechanized Agriculture, Xinjiang Academy of Agricultural Sciences, Urumqi 830091, China; xin0821h@163.com (X.H.); cyfgunman@163.com (Y.C.)

² College of Water Resources and Civil Engineering, China Agricultural University, Beijing 100083, China; rizwan3147@gmail.com

* Correspondence: yhm_shz@163.com (H.Y.); 15612771262@163.com (Y.Z.)

Abstract: Droplet impact angle and shear stress are important indicators of surface runoff under sprinkler irrigation, and determining the distribution characteristics of these two indicators on sloping land is of great significance for preventing soil surface erosion. Therefore, three slopes (0, 10%, and 20%) and two directions (uphill and downhill) under a Rainbird LF1200 rotary sprinkler were considered in this study. The distribution of droplet impact angles and shear stresses along the radial direction were investigated under various working conditions. The correlations among the droplet impact angle, shear stress, and distance from the sprinkler were also analyzed. These results indicated that the closer to the sprinkler, the larger the droplet impact angle and the smaller the shear stress, and the two indicators gradually decreased and increased with the increase of distance from the sprinkler, respectively. Accordingly, there was a very high potential for soil surface runoff at the spray jet end. It was also observed that the uphill direction generally had a greater impact angle and less shear stress than flat land, while the downhill direction had exactly the opposite result. However, regardless of the direction, an increase in the slope could intensify its effect on the droplet shear stress and impact angle. Therefore, there is an urgent need to focus on the occurrence of surface runoff in soils with larger slopes. In addition, two radial droplet shear stress distribution models were developed, and it was verified that Model 2 had higher accuracy ($MAE = 176.6 \text{ N m}^{-2}$, $MBE = 32.8 \text{ N m}^{-2}$, and $NRMSE = 14.4\%$) and could be used to predict the average droplet shear stresses at different slopes, directions, and distances from the sprinkler. This study contributes to the soil erosion prevention and the sprinkler irrigation system optimization on sloping land.

Keywords: sprinkler irrigation; sloping land; impact angle of droplet; shear stress of droplet; model



Citation: Hui, X.; Chen, Y.; Shoukat, M.R.; Yang, H.; Zheng, Y. Sprinkler Irrigation on Sloping Land: Distribution Characteristics of Droplet Impact Angle and Shear Stress. *Water* **2024**, *16*, 60. <https://doi.org/10.3390/w16010060>

Academic Editors: Giuseppe Oliveto and Saseendran S. Anapalli

Received: 18 September 2023

Revised: 29 October 2023

Accepted: 21 December 2023

Published: 23 December 2023



Copyright: © 2023 by the authors. Licensee MDPI, Basel, Switzerland. This article is an open access article distributed under the terms and conditions of the Creative Commons Attribution (CC BY) license (<https://creativecommons.org/licenses/by/4.0/>).

1. Introduction

By 2021, there were approximately 29.3 million hectares of cultivated land in China with slopes above 6°, accounting for 22.74% of the total cultivated land area. These sloping lands provide an important cultivation base for grain, vegetable, and fruit for the farmers in hills or mountains of China [1–3]. However, affected by the terrain slope, the sloping land usually has poor soil water retention capacity, making it prone to drought and greatly reducing crop yield and quality [4–6]. Therefore, selecting a reasonable irrigation method for the timely and appropriate irrigation of crops is crucial.

As a widely accepted irrigation method, sprinkler irrigation has been successfully applied on sloping land due to its strong adaptability to terrain slope and its high water utilization efficiency [7,8]. However, the sprinkler droplets that continue to hit the soil can easily cause soil surface sealing, resulting in surface runoff on sloping land and affecting the absorption of water by crops [9,10]. Results from previous studies have suggested that soil surface sealing is mainly due to the separation of soil particles from aggregates [11,12], and it is generally considered to be closely related to sprinkler droplet kinetic energy [13–16].

Nevertheless, some scholars believed from the perspective of mechanism that the separation of soil particles was actually attributed to the droplet shear stress on the soil surface, rather than the droplet kinetic energy [17–19]. Taken together, it is of great significance to determine the distribution characteristics of droplet shear stresses under sprinkler irrigation on sloping land.

Several studies have been carried out on the distribution characteristics of droplet impact angles and shear stresses under sprinkler irrigation. Chang and Hills [20] developed a numerical model and simulated the droplet shear stress distributions on the soil surface based on the full three-dimensional (3D) Navier–Stokes equations and finite difference procedure. They found that compared to the vertical droplet impact, the oblique droplet impact increased the shear stress. Meanwhile, Chang and Hills [18] carried out a laboratory experiment to further evaluate the sprinkler droplet impact angles affecting the soil infiltration. The results showed that the steady infiltration rates of the soil sequentially increased with an increase in the impact angle. The above results indicate that the droplet impact angle of the sprinkler has a considerable influence on the distribution of shear stresses and soil infiltration, which inevitably affects the growth of crops. However, their study only considered three droplet impact angles (45°, 60°, and 90°), which is not in line with the actual impact of droplets on the soil at multiple angles during sprinkler irrigation. Therefore, Hui et al. [21] used a two-dimensional video disdrometer (2DVD) to investigate the droplet impact angle distributions of a ball-driven sprinkler and established the relationships between droplet impact angles and shear stresses. Moreover, Hui et al. [16] also selected the three low-pressure sprinkler types, i.e., Nelson D3000, R3000, and Komet KPT, for research and observed that with the increase of distance from the sprinkler, the droplet impact angle decreased and velocity increased, which resulted in a significant enlargement in the shear stress. These aforementioned research results provide another scientific method for accurately predicting soil erosion and designing irrigation engineering under sprinkler irrigation. Nonetheless, this research has primarily focused on flat land, with less reports on sloping land. If the distribution data regarding impact angles and shear stresses of the droplets on flat land are used for the sprinkler irrigation systems optimization and the soil erosion prevention on sloping land, they are bound to cause large errors. Moreover, considering that slope sprinkler irrigation is more likely to generate surface runoff and aggravate soil erosion than flat irrigation, it is necessary to analyze the impact angle and shear stress of sprinkler droplets on sloping land.

The purpose of this research was to study the distribution characteristics of droplet impact angles and shear stresses of a Rainbird LF1200 rotary sprinkler with slopes of 0, 10%, and 20% in the uphill and downhill directions. Specifically, the following aspects were carried out: (1) to assess the droplet impact angle distributions along the radial direction on sloping land; (2) to analyze the relationships among the droplet impact angle, shear stress, and distance from the sprinkler, as well as the relationship between the droplet impact angle and shear stress; and (3) to develop and verify calculation models for the radial droplet shear stress distribution.

2. Materials and Methods

2.1. Experimental Setup

Under indoor windless conditions, a distribution experiment of droplets of an individual sprinkler on sloping land was performed. The slope surface in the test was manually constructed with steel plates and adjustable height brackets, which could be dynamically adjusted according to different slope requirements. The sprinkler tested in the experiment was a rotating sprinkler (LF1200, Rain Bird Corp., Azusa, California, USA), as shown in Figure 1. The LF1200 sprinkler has a small flow rate, but its robust construction can withstand a wide range of harsh conditions in agricultural applications. These advantages make it widely used in agricultural irrigation [22,23]. Although there are 4 brackets on the sprinkler, they are successfully evaded during the test of the droplets, so the droplet measurement results were not affected. A nozzle diameter of 2.18 mm and a jet

angle of 17° were selected for this sprinkler, and its working pressure ranged from 170 to 410 kPa. The LF1200 sprinkler was mounted on an adjustable height riser with a manual valve and a pressure transducer with a range of 0 to 500 kPa (CYB, accuracy of $\pm 0.1\%$, Xi'an Xinmin Electronic Technology Co., Ltd., China) to regulate and monitor the sprinkler inlet operating pressure. We then recorded the pressure every 5 s and calculated the average value at the end of each test. Furthermore, an IS80–50–250 centrifugal pump (Foshan Pump Factory Co. Ltd., Foshan, China) was applied to pressurize the water to the sprinkler inlet. An EMF 5000 electromagnetic flowmeter with an accuracy of 0.5% was used to measure the real-time flow rate in the pipeline.



Figure 1. Sprinkler used in the experiment.

In addition, a two-dimensional video disdrometer (2DVD, Joanneum Research Corp, Graz, Austria) was used to obtain the sprinkler droplet information (Figure 2). This equipment includes an indoor user terminal, a power supply unit, and a measurement device and is often used for measuring the various precipitation particles. A 2DVD can measure the size, shape, aggregation state, falling velocity, and direction of individual precipitation particles, such as rain, snow, and hail in real time. It is widely applied in meteorology and the environment, telecommunications, wave propagation, industrial applications, and other fields [24]. In the droplet distribution test of sprinklers on sloping land, the droplets passing through the measurement area ($100 \times 100 \text{ mm}^2$) were continuously scanned by the two perpendicularly disposed charge-coupled device (CCD) cameras, and then each droplet velocity perpendicular and parallel to the slope surface was recorded [25,26].

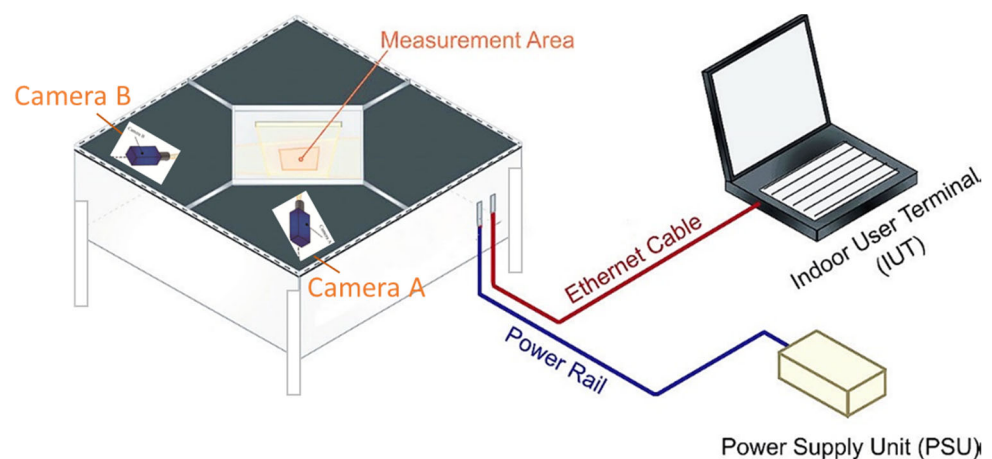


Figure 2. Droplet measuring device used in the experiment.

2.2. Experimental Design

Three slopes (0, 10%, and 20%) were considered in the droplet distribution test of the LF1200 rotating sprinkler. Each slope was divided into two directions: uphill and downhill. There was a total of six trials, and each trial was repeated three times to obtain more accurate experimental data. In the droplet test of the sprinkler, the sprinkler operating pressure was maintained at 300 kPa, which is the designed pressure. The indoor relative

humidity was about 65%, and air and water temperatures were approximately 33 °C and 29 °C, respectively. In the experiment, the ISO 7749-2 [27] and ISO 15886-3 [28] standards were adopted.

To maintain similarity to the installation heights of sprinklers used in most solid-set sprinkler irrigation engineering, the sprinkler in the test was adjusted to 1 m above the cameras of the 2DVD instrument before each trial [29]. Subsequently, the centrifugal pump and manual valves were successively turned on, and the droplet velocity information was collected by the 2DVD under the stable operating pressure and flow rate of the sprinkler. The sprinkler droplet measuring points were arranged at intervals of 2 m along the uphill or downhill direction, where the first measuring point was 1 m from the sprinkler on sloping land (Figure 3). The test did not arrange a measuring point every 1 m such as with flat land, mainly because the workload of droplet testing on sloping land was much larger than that on flat land. Approximately 1000 effective droplets were obtained at each measuring point. The error in the data caused by droplet splashing was checked and eliminated with a 3σ criterion (Pauta criterion that is one of the criteria for checking erroneous data) after all droplet data were collected [30].

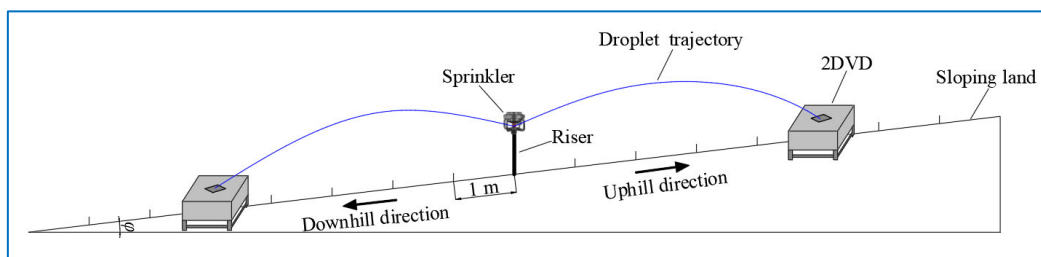


Figure 3. Droplet distribution test for the sprinkler irrigation on sloping land.

2.3. Calculation Method

The droplet velocities perpendicular and parallel to the slope surface were used to calculate the resultant droplet velocity (hereafter referred to as droplet velocity). The calculation formula is as follows:

$$V = \sqrt{V_e^2 + V_a^2} \quad (1)$$

where V is the resultant droplet velocity (m s^{-1}); V_e is the velocity of the droplet perpendicular to the slope surface (m s^{-1}); V_a is the velocity of the droplet parallel to the slope surface (m s^{-1}).

The angle between the direction of the droplet impacting the slope and the slope surface is the droplet impact angle. The calculation formula is as follows:

$$\theta = \frac{180}{\pi} \arctan\left(\frac{V_e}{V_a}\right) \quad (2)$$

where θ is the droplet impact angle ($^\circ$).

The droplet shear stress on sloping land was calculated using Equation (3) [31]:

$$S_s = \frac{1}{2} \rho V_a^2 \quad (3)$$

where S_s is the droplet shear stress (N m^{-2}); ρ is the droplet mass density (kg m^{-3}).

2.4. Data Analysis

The relationships among the droplet impact angle, shear stress, and distance from the sprinkler, as well as the relationship between the droplet impact angle and shear stress, were developed by the regression analysis using Origin 2022 (OriginLab, Northampton, MA,

USA). The goodness of fit of these regression relationships was assessed by the coefficient of determination (R^2). A higher R^2 value reflects a higher goodness of fit. Based on the above relationships, the radial distribution models of droplet shear stresses were proposed by stepwise regression analysis. The accuracy of these distribution models was verified by the mean absolute error (MAE), mean bias error (MBE), and normalized root mean square error (NRMSE) between the simulated and measured values. The lower the error values, the more accurately the models predict droplet shear stress. This is a common method to determine the feasibility of models.

3. Results and Analysis

3.1. Radial Droplet Impact Angle Distribution on Sloping Land

Different droplet impact angles can result in different shear stresses, which in turn affect the soil erosion on sloping land [32]. Figure 4 shows the radial distribution characteristics of droplet impact angles under the three slopes in uphill and downhill directions. It was observed that regardless of the slope and direction, more than 45% of droplet impact angles were distributed between 80° and 90° at 1 m from the sprinkler on sloping land. This result indicates that the impact angles of most droplets near the sprinkler were close to perpendicular to the slope surface, thus resulting in relatively weak soil erosion. Similar outcomes in sprinkler irrigation experiments on flat land have been observed by other researchers [18,21,33]. This was expected because small diameter droplets predominate near the sprinkler [16,34,35]. Meanwhile, the specific surface area (surface area per unit volume) of the small droplet is large [36]; therefore, its air friction resistance ratio is relatively high, and the horizontal droplet velocity rapidly approaches zero [37]. Consequently, the small diameter droplets traveled short distances horizontally, and their impact angles were nearly perpendicular to the soil surface with a small slope.

As the distance from the sprinkler on sloping land increased, the decrease in the proportion of small diameter droplets led to a general reduction in the impact angles of droplets. The number of droplets at $80\text{--}90^\circ$ impact angles under various slopes and directions decreased when the distance increased to 3 m, and those of the droplets between 70° and 80° increased. Taking the downhill with a slope of 10% as an example, the relative frequency of droplets at $80\text{--}90^\circ$ decreased from 49.7% at a distance of 1 m to 32.9% at 3 m, while that at $70\text{--}80^\circ$ increased from 26.0% at 1 m to 36.9% at 3 m. With a further enlargement in distance from the sprinkler on sloping land, the proportion of larger droplet impact angles continued to decrease, and that of smaller droplets correspondingly increased. As the distance increased to 5 m, the relative frequency of droplets above 70° under three slopes and two directions tapered off by an average of 6.9% on the basis of 3 m. Until the distance reached the spray jet end, a large number of droplet impact angles began to appear in the range of $30\text{--}50^\circ$, and the droplet relative frequency in this range even accounted for 23.4% under the downhill with a slope of 20%. These findings signified that the distance from the sprinkler on sloping land had a significant negative effect on the distribution of droplet impact angles [33]. Meanwhile, it can be seen from Figure 5 that the relationship between the droplet impact angle and velocity was close, which indicates that the droplet impact angle decreased with the increase in the velocity. Therefore, it could be inferred that the largest droplet shear stress mainly occurred at the end of the spray jet. In addition, it was not difficult to find that the farther distance from the sprinkler on sloping land was associated with a more dispersed droplet impact angle, which suggested that the spray jet end might also be the area where droplets collided most violently with each other. This result is consistent with the droplet diameter distributions obtained by Hui et al. [21] using a ball-driven sprinkler and Hui et al. [33] using low-pressure sprinklers.

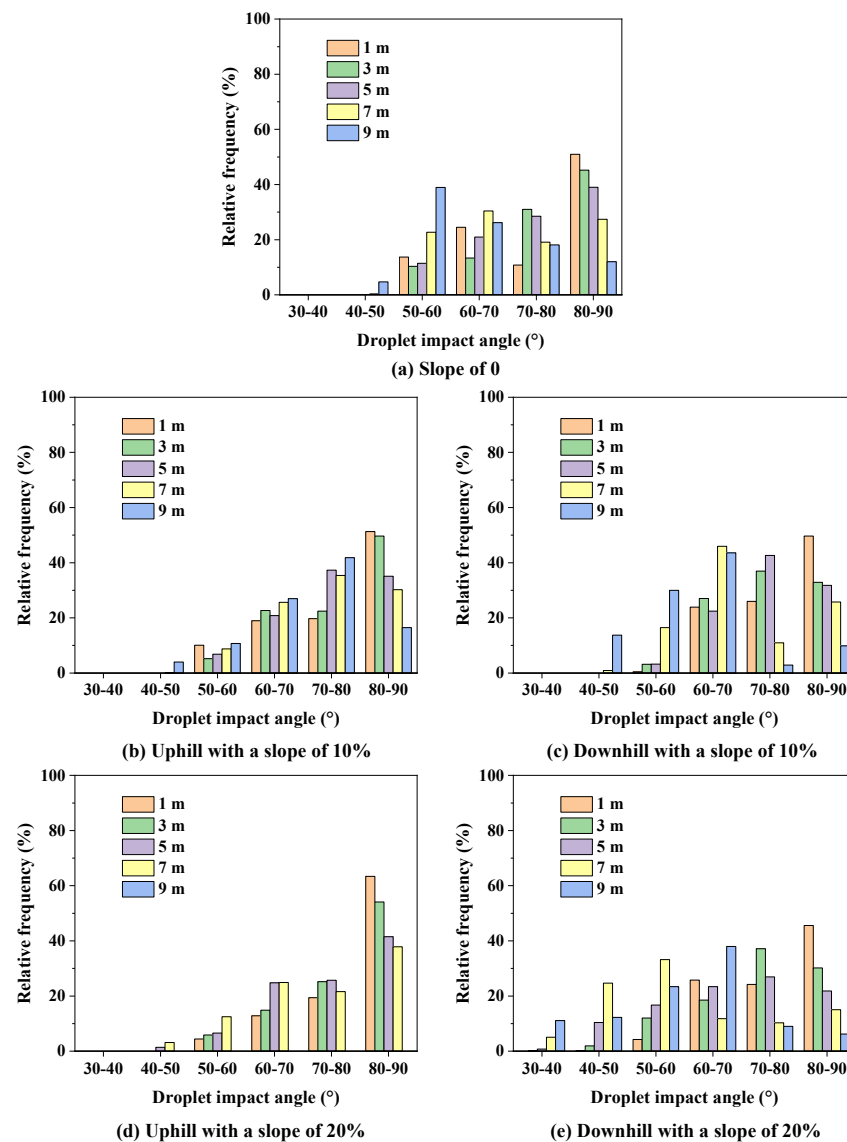


Figure 4. Radial distribution characteristics of the droplet impact angles under three slopes in uphill and downhill directions.

Furthermore, it can be observed from Figure 4 that the droplet impact angle distribution varies with slope and direction. For example, for the slopes of 0, 10%, and 20% in the uphill direction, the average relative frequencies in the droplet impact angle range of 30–60° under the five distances from the sprinkler were 20.5%, 9.1%, and 8.5%, respectively, while the corresponding values in the 80–90° impact angle range under different slopes were 34.9%, 36.6%, and 49.2%, respectively. In the downhill direction, the above relative frequency values of 0, 10%, and 20% were changed to 20.5%, 13.6%, and 31.2% for 30–60° and 34.9%, 30.0%, and 23.8% for 80–90°, respectively. These results indicate that the uphill direction had a generally positive influence on the distribution of larger impact angles of droplets, while its influence on the distribution of smaller droplet impact angles was negative. A reverse outcome was obtained in the downhill direction. Nonetheless, irrespective of the uphill or downhill direction, the influence of slope on the impact angle became more obvious with an increase in the slope. Therefore, the potential droplet shear stress of the uphill slope was smaller relative to the flat land, and that of the downhill slope was larger, so the higher the slope, the more attention should be paid to the occurrence of soil surface erosion [5].

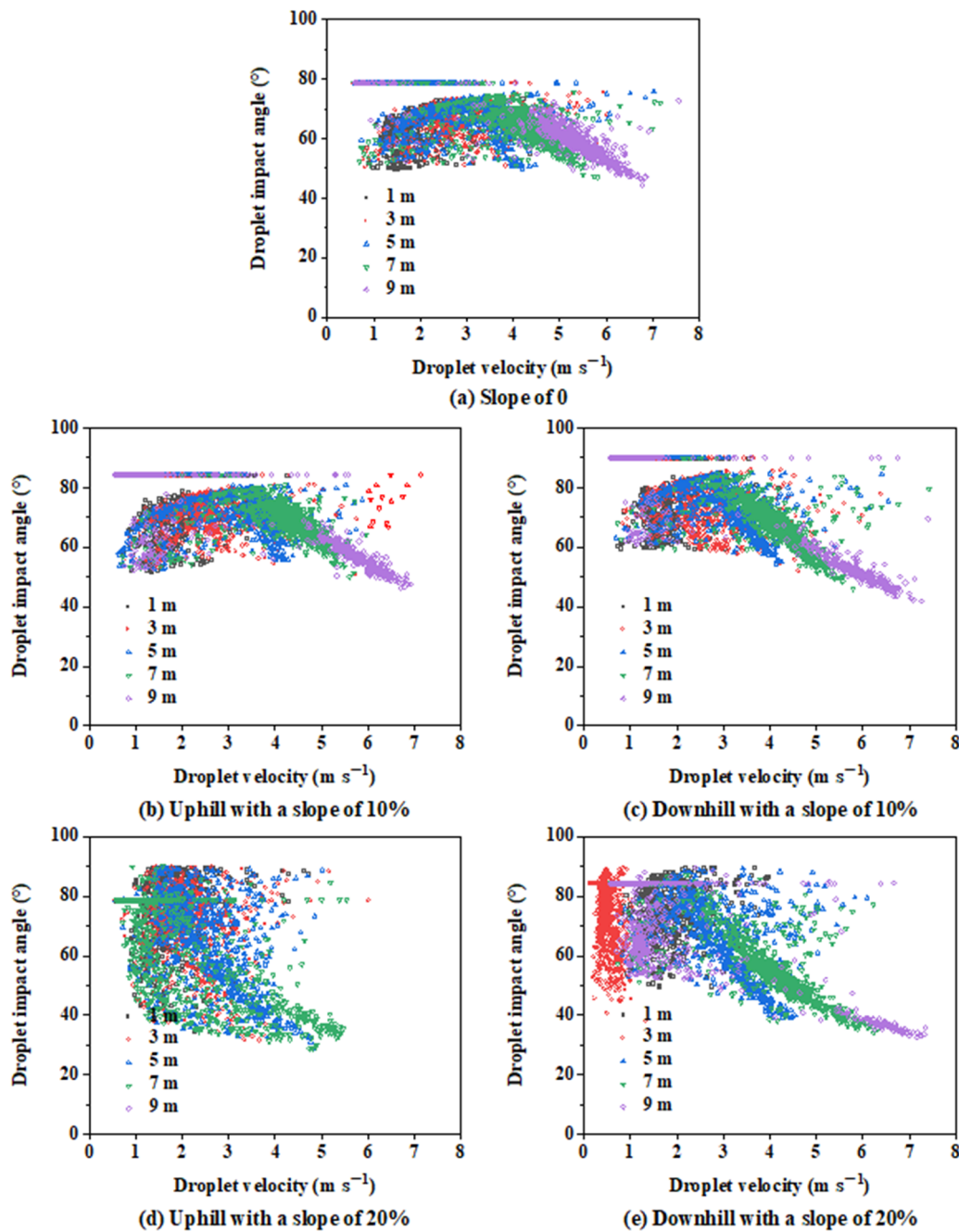


Figure 5. Relationships between the droplet velocities and impact angles under three slopes in uphill and downhill directions.

3.2. Relationship between Droplet Impact Angle and Distance from Sprinkler on Sloping Land

To further investigate the relationship between droplet impact angle and distance from the sprinkler on sloping land, Figure 6 shows the radial distribution characteristics of average droplet impact angles under the three slopes in uphill and downhill directions. Similar to the results of the droplet relative frequency distribution mentioned earlier, with an increase in distance from the sprinkler, the average droplet impact angle decreased, irrespective of the slope or direction. As shown in Figure 6, for the uphill direction, the average impact angles at different distances on three slopes were distributed between 63.8° and 78.3°, while the range of average droplet impact angles corresponding to the downhill direction was 56.9–75.9°. This outcome suggests that the average impact angles in the uphill were generally greater than those in the downhill. This was not surprising because when

the sprinkler sprayed uphill, the water jet trajectory was blocked by the slope, resulting in the early landing of droplets. Thus, the droplet impact angles became larger than those of the flat land. When the sprinkler was sprayed downhill, due to the slope, the landing time of the jet trajectory was delayed compared with the flat land, which led to a reduction in droplet impact angles. From the schematic diagram depicted in Figure 7, the impact angle of a droplet sprayed downhill is always smaller than that sprayed uphill, that is, $\alpha < \beta$. In addition, it was not difficult to find that in the uphill, the larger the slope, the greater the average impact angle, and in the downhill, the larger slope was associated with a smaller average impact angle. The maximum differences in average impact angle between the three slopes (0, 10%, and 20%) at the same distance from the sprinkler were 4.9° and 7° for the uphill and downhill, respectively.

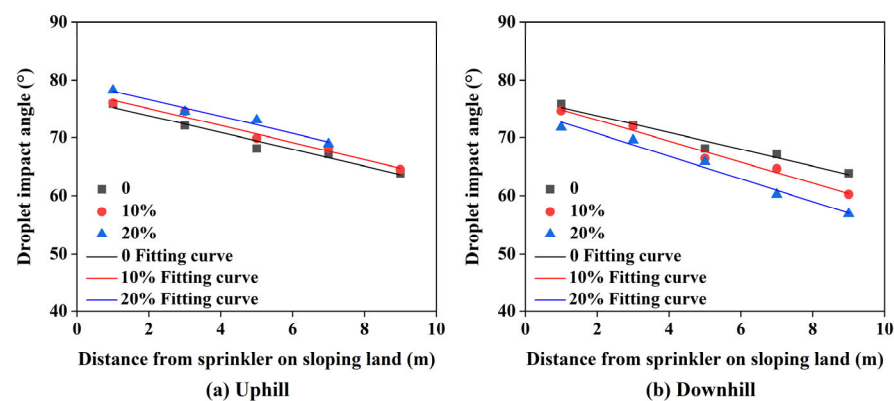


Figure 6. Radial distribution characteristics of the average droplet impact angles under three slopes in uphill and downhill directions.

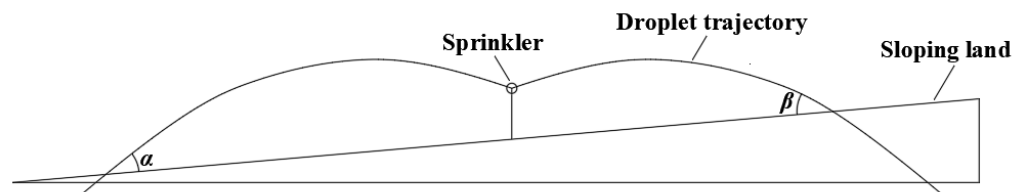


Figure 7. Schematic diagram of the impact angle of droplets sprayed uphill and downhill. Note: α represents the impact angle of a droplet sprayed downhill and β represents the impact angle of a droplet sprayed uphill.

Furthermore, regression analysis showed that a linear relationship existed between the average droplet impact angle and distance from the sprinkler, in line with the results obtained by Hui et al. [21] with a ball-driven sprinkler. The linear equations for various slopes and directions can be uniformly expressed by $\bar{\theta} = al + b$. Table 1 shows that the R^2 values under various working conditions were greater than 0.96, indicating that the goodness of fit of these equations is excellent and has strong universality. To determine the mathematical relationships among average droplet impact angle, slope, and distance from the sprinkler in the two directions, the relationships between the slope and coefficients a and b were first developed and then integrated to propose the following equations:

$$\text{Uphill : } \bar{\theta} = (-0.155s - 1.4508)l + 14.65s + 76.6 \tag{4}$$

$$\text{Downhill : } \bar{\theta} = (-2.535s - 1.4848)l - 10.285s + 76.988 \tag{5}$$

where $\bar{\theta}$ is the average impact angle of the droplet ($^\circ$); s is the slope (%); l is the distance from the sprinkler (m).

Table 1. Fitting equations between the average droplet impact angles ($\bar{\theta}$) and distances from sprinkler (l) under the three slopes in uphill and downhill directions.

Slope Direction	Slope Value	Fitting Coefficient		R^2
		a	b	
Uphill	0	−1.448	76.653	0.969
	10%	−1.472	77.960	0.970
	20%	−1.479	79.583	0.973
Downhill	0	−1.448	76.653	0.969
	10%	−1.812	76.629	0.975
	20%	−1.955	74.596	0.975

Note: a and b represent the coefficients of the fitting equation $\bar{\theta} = al + b$.

3.3. Relationship between Droplet Impact Angle and Shear Stress on Sloping Land

The shear stress of the droplet directly affects the soil surface crusting and is one of the main factors in soil erosion [38]. Figure 8 depicts the relationships between droplet impact angles and shear stresses under the three slopes in uphill and downhill directions. Overall, larger droplet impact angles corresponded to weaker droplet shear stresses, and smaller impact angles corresponded to stronger shear stresses. This result has been confirmed in many studies on flat land [20,21,33]. Nonetheless, the shear stresses of some droplets were basically unchanged, and their values were very small. This might be because the velocities of these droplets were already small and tended to increase as the impact angles increased. According to statistics, the droplet shear stresses under a slope of 0, uphill with slopes of 10% and 20%, and downhill with slopes of 10% and 20% were distributed at 6.0–11,742.7, 1.6–10,920.5, 0–10,202.6, 0–14,606.8, and 0–18,597.7 N m^{−2}, respectively. It was found from the above data that the minimum droplet shear stress under each slope and direction was close to 0, and the difference between various treatments was mainly reflected in the maximum shear stress. That is, the greater the slope in the uphill, the smaller the maximum shear stress, and a reverse trend between the droplet shear stress and slope was observed in the downhill. This is consistent with the previous results regarding the distribution of the droplet impact angles, as shown in Figure 4.

Due to the close correlation between the droplet shear stress and impact angle, the change in distance from the sprinkler also resulted in various variations in shear stress distribution. Unsurprisingly, the minimum shear stresses under various treatments were mainly distributed near the sprinkler, while the maximum were mainly at the spray jet end (Figure 4). The ranges of shear stresses under the slope of 0, uphill with slopes of 10% and 20%, and downhill with slopes of 10% and 20% were 6.2–3049.3, 1.6–1141.8, 0–2234.6, 0–1155.2, and 0–1549.4 N m^{−2}, respectively, for 1 m from the sprinkler and 6.5–11,742.7, 1.6–10,920.5, 0–10,202.6, 0–14,606.8, and 0.2–18,597.7 N m^{−2}, respectively, for 9 m from the sprinkler (only 7 m in uphill with a slope of 20%).

In addition, it is important to note from the regression analysis that droplet shear stresses and impact angles under three slopes and two directions had obvious exponential relationships, which could be expressed by $S_s = ce^{d\theta}$. These results do not coincide with the polynomial relationship between the two indicators obtained by Hui et al. [33] using a low-pressure sprinkler on flat land. This also implies a stronger regularity between these two indicators under the influence of the slope, and it could be observed from Table 2 that the average R^2 value under various treatments was 0.879. Equations (6) and (7) present the relationships among droplet shear stress, impact angle, and slope in the two directions, respectively, as follows:

$$\text{Uphill : } S_s = \left(-2 \times 10^{6s} + 564738 \right) e^{(-0.03s - 0.0933)\theta} \quad (6)$$

$$\text{Downhill : } S_s = \left(2 \times 10^{6s} + 612917 \right) e^{(-0.165s - 0.0838)\theta} \quad (7)$$

where S_s is the shear stress of the droplet (N m^{-2}); θ is the impact angle of the droplet ($^\circ$); s is the slope (%).

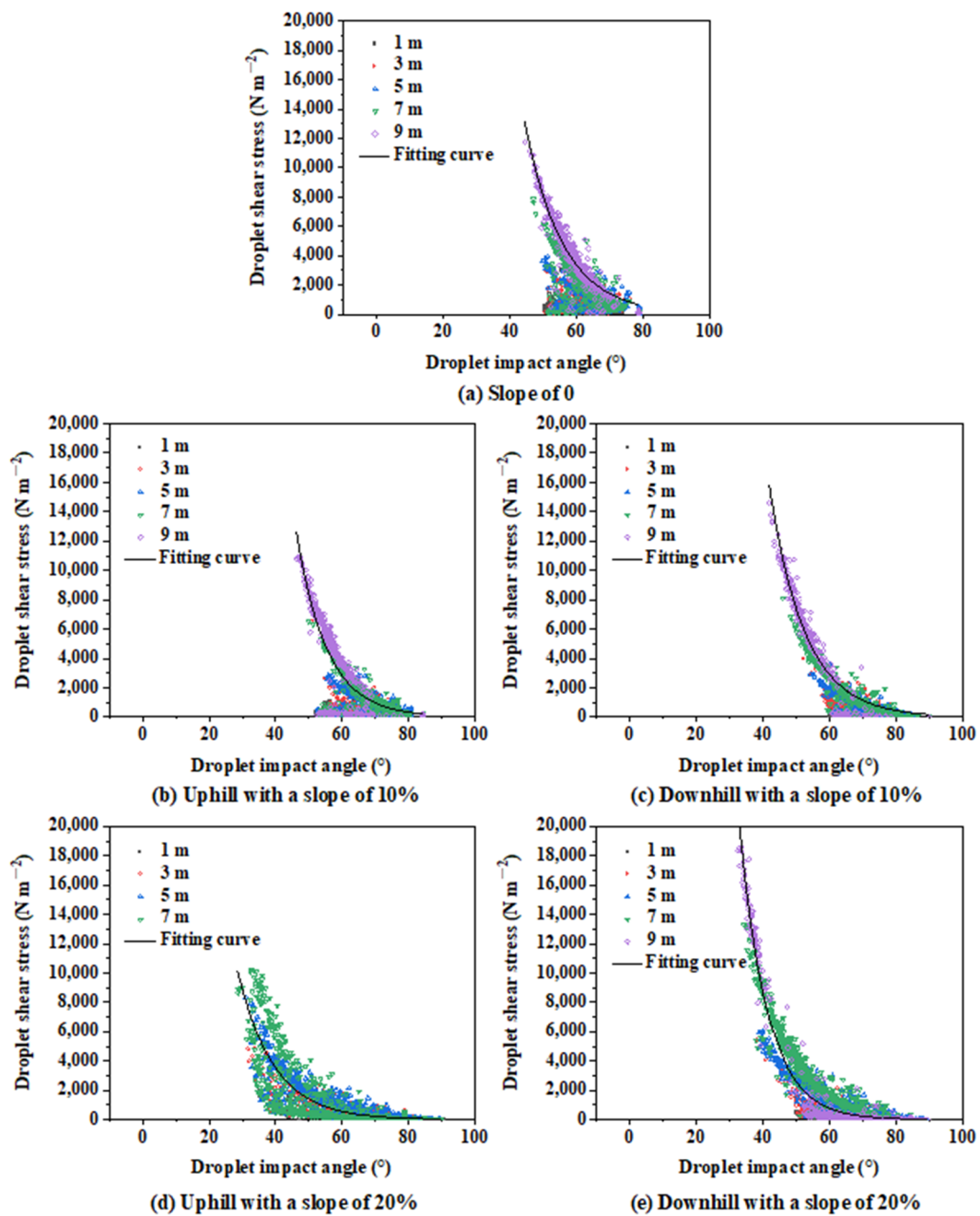


Figure 8. Relationships between the droplet impact angles and shear stresses under three slopes in uphill and downhill directions.

3.4. Relationship between Droplet Shear Stress and Distance from Sprinkler on Sloping Land

The relationship between the distance from the sprinkler and average droplet shear stress reflects the overall distribution of shear stresses. Figure 9 shows the radial distribution characteristics of average droplet shear stresses under the three slopes in uphill and downhill directions. As expected, the average shear stress tended to increase as the distance from the sprinkler increased. In the uphill direction, the average shear stresses along the radial direction ranged from 120.6 to 3077.4, 97.3 to 2772.6, and 87.9 to 1339.5 N m^{-2} under slopes of 0, 10%, and 20%, respectively. The corresponding average shear stress ranges in

the downhill were 120.6–3077.4, 169.5–3130.7, and 190.7–3826.8 N m⁻², respectively. These data illustrated two points. One point was that in the uphill, the larger slope resulted in a lower average droplet shear stress, while the opposite results were obtained in the downhill. This was mainly due to the influence of slope on the spray jet trajectory, which caused the shear stress distribution in uphill and downhill directions to vary. Another point was whether it was uphill or downhill, and the smaller difference in average shear stress between each slope occurred when the distance was closer to the sprinkler. This difference became more apparent as the distance from the sprinkler increased, reaching a maximum at the end of the spray jet. Taken together, when carrying out the prevention of soil erosion in slope sprinkler irrigation, it was necessary to consider the spray jet end. This finding is consistent with the recommendations of several scholars from the perspectives of droplet kinetic energy, water application rate, and specific power [5,39,40].

Table 2. Fitting equations between the droplet impact angles (θ) and shear stresses (S_s) under three slopes in uphill and downhill directions.

Slope Direction	Slope Value	Fitting Coefficient		R^2
		c	d	
Uphill	0	627,715.655	−0.087	0.908
	10%	196,231.670	−0.109	0.815
	20%	142,614.300	−0.093	0.695
Downhill	0	627,715.655	−0.087	0.908
	10%	802,688.077	−0.094	0.970
	20%	1,066,449.740	−0.120	0.979

Note: c and d represent the coefficients of the fitting equation $S_s = ce^{d\theta}$.

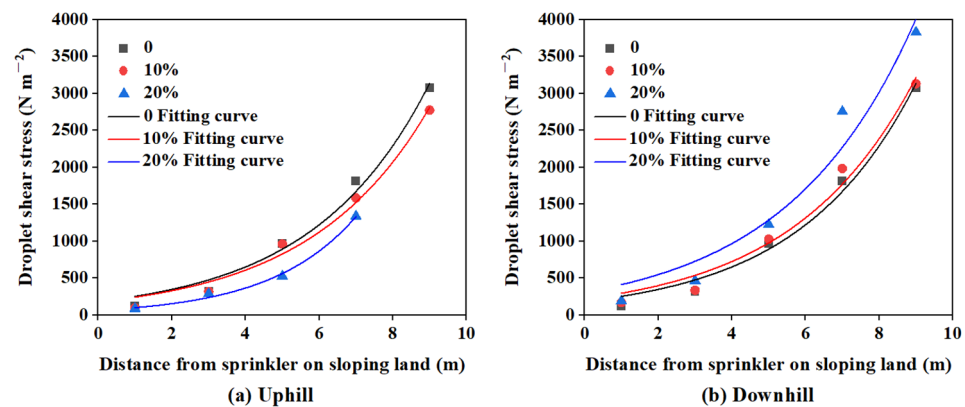


Figure 9. Radial distribution characteristics of the average droplet shear stresses under three slopes in uphill and downhill directions.

Similarly, Figure 9 shows a regression analysis between the distance from the sprinkler and average shear stress under three slopes and two directions. The results showed that the two indicators exhibited an excellent exponential relationship under all working conditions (mean $R^2 = 0.984$; Table 3). To facilitate the calculation of average shear stresses at different slopes and distances from the sprinkler, the following two equations propose the relationships among average shear stress, slope, and distance from the sprinkler in the two directions:

$$\text{Uphill : } \bar{S}_s = (-599.99s + 203.18)e^{(0.585s+0.2918)l} \tag{8}$$

$$\text{Downhill : } \bar{S}_s = (624.85s + 176)e^{(-0.15s+0.3137)l} \tag{9}$$

where \bar{S}_s is the average shear stress of the droplet (N m⁻²); s is the slope (%); l is the distance from the sprinkler (m).

Table 3. Fitting equations between the average droplet shear stresses (\bar{S}_s) and distances from sprinkler (l) under three slopes in uphill and downhill directions.

Slope Direction	Slope Value	Fitting Coefficient		R^2
		f	g	
Uphill	0	185.369	0.314	0.988
	10%	178.798	0.306	0.987
	20%	65.371	0.431	0.996
Downhill	0	185.369	0.314	0.988
	10%	219.744	0.298	0.982
	20%	310.338	0.284	0.960

Note: f and g represent the coefficients of the fitting equation. $\bar{S}_s = fe^{gl}$.

3.5. Radial Distribution Model of Droplet Shear Stresses on Sloping Land

The development of a radial distribution model of the shear stresses on sloping land can scientifically predict the average droplet shear stresses at different slopes, directions, and distances from the sprinkler. This is of great significance for the soil erosion prevention and the sprinkler irrigation systems optimization on sloping land. Figure 10 illustrates the flowchart of two droplet shear stress distribution models calculated from the above fitting equations. The specific calculation process of Model 1 was as follows: first, setting the distance from the sprinkler (l) and slope (s), then selecting Equations (4) and (5) to calculate the average droplet impact angles (θ) in uphill and downhill directions, respectively, and finally obtaining the average droplet shear stresses (\bar{S}_s) by Equations (6) and (7). The calculation process of Model 2 was relatively simple; that is, the distance from the sprinkler (l) and slope (s) were directly brought into Equations (8) and (9) to acquire the average droplet shear stresses (\bar{S}_s) in uphill and downhill directions, respectively.

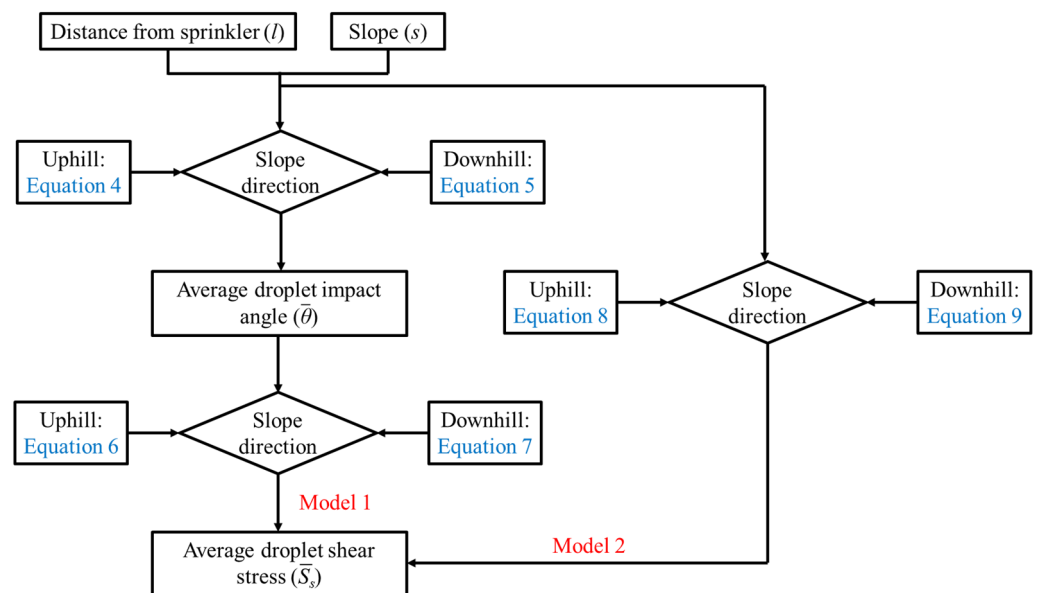


Figure 10. Flowchart for developing the droplet shear stress distribution models on sloping land. Note: The blue font represents the equation used and the red font represents the model developed.

To verify the accuracy of these models, Figure 11 shows a comparison of simulated and measured values of the two droplet shear stress distribution models under different working conditions. It is clear that the accuracy of Model 2 was superior to that of Model 1. The MAE, MBE, and NRMSE values were 156.0 N m⁻², 49.7 N m⁻², and 20.3% for uphill, respectively, and 176.6 N m⁻², 32.8 N m⁻², and 14.4% for downhill, respectively. These results revealed that the accuracy of Model 2 was at a fair level on the uphill, while that on

the downhill reached a good level [41]. Consequently, Model 2 developed in this study is feasible for the prediction of radial droplet shear stress distribution on sloping land under a Rainbird LF1200 sprinkler with the nozzle diameter of 2.18 mm and operating pressure of 300 kPa. However, this study has certain limitations. Firstly, the model was only proposed using the LF1200 rotary sprinkler under three slopes and two directions. In fact, there are many types of rotary sprinklers, LF1200 is only one of the common ones, and the actual sloping land has a variety of slopes and directions. Secondly, multi-sprinkler combination is often used in the design of irrigation engineering, so at the same point there may be droplet shear stresses from multiple slope directions and distances from the sprinkler. Therefore, it is necessary to further propose a more general droplet shear stress distribution model on sloping land.

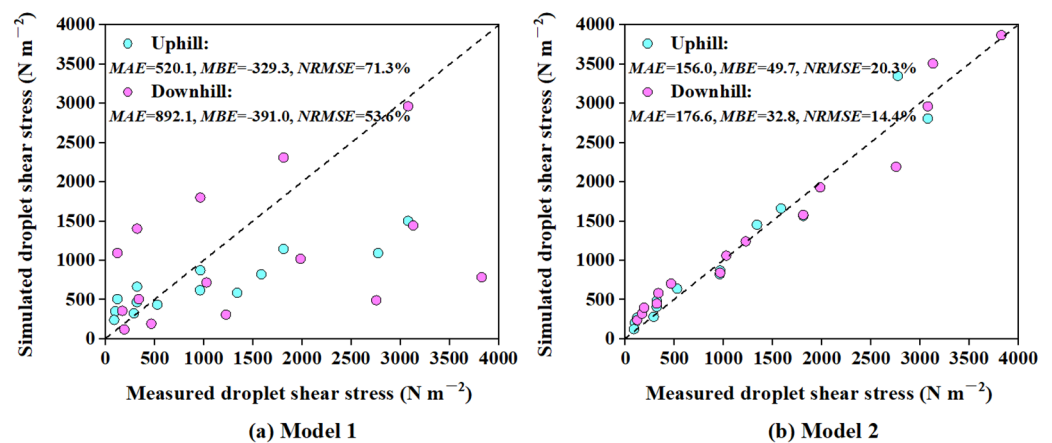


Figure 11. Measured and simulated results comparisons obtained by two droplet shear stress distribution models. Note: The dashed line represents a 1:1 line.

4. Conclusions

Regardless of the slope and direction, the larger impact angle and smaller shear stress of the droplet were mainly distributed near the sprinkler, and with the increase in distance from the sprinkler, the droplet impact angle gradually decreased and the shear stress increased correspondingly. As a result, the soil erosion at the end of the spray jet is likely to be the most severe on sloping land. In addition, the slope and direction significantly affected the impact angle and shear stress of the droplet. Compared with flat land, the smaller shear stresses and larger impact angles generally occurred in the uphill direction, and the reverse result was obtained in the downhill. However, in the uphill or downhill directions, the effect of increasing the slope on the droplet shear stress and impact angle intensified. Therefore, more attention needs to be paid to surface runoff on steep slopes.

This study developed the two radial distribution models of droplet shear stresses on sloping land. It was found through verification that Model 2 had better accuracy ($MAE = 176.6 \text{ N m}^{-2}$, $MBE = 32.8 \text{ N m}^{-2}$, and $NRMSE = 14.4\%$), which could be used to predict the average droplet shear stresses at different slopes, directions, and distances from the sprinkler. The construction of this model could provide help for preventing soil erosion and designing sprinkler irrigation engineering on sloping land.

Author Contributions: X.H.: Data analysis, Chart drawing, Article writing. M.R.S.: Data processing. Y.C.: Data processing. H.Y.: Experimental design, Thesis revision. Y.Z.: Experimental design, Thesis revision. All authors have read and agreed to the published version of the manuscript.

Funding: This research was funded by the Academy of Agricultural Sciences Youth Science and Technology Backbone Innovation Ability Training Project (XJNKQ-2023026; XJNKQ-2020018); National Natural Science Foundation of China (52309071).

Data Availability Statement: Data will be available on request.

Conflicts of Interest: The authors declare no conflict of interest.

References

- Wang, Y.; Yang, C.; Zhang, Y.; Xue, Y. Mountainous areas: Alleviating the shortage of cultivated land caused by Changing dietary structure in China. *Land* **2023**, *12*, 1464. [\[CrossRef\]](#)
- Li, H.; Wu, Y.; Huang, X.; Sloan, M.; Skitmore, M. Spatial-temporal evolution and classification of marginalization of cultivated land in the process of urbanization. *Habitat Int.* **2017**, *61*, 1–8. [\[CrossRef\]](#)
- Sun, X.; Li, F. Spatiotemporal assessment and trade-offs of multiple ecosystem services based on land use changes in Zengcheng, China. *Sci. Total Environ.* **2017**, *609*, 1569–1581. [\[CrossRef\]](#) [\[PubMed\]](#)
- Wolka, K.; Mulder, J.; Biazin, B. Effects of soil and water conservation techniques on crop yield, runoff and soil loss in Sub-Saharan Africa: A review. *Agric. Water Manag.* **2018**, *207*, 67–79. [\[CrossRef\]](#)
- Zhang, L.; Hui, X.; Chen, J. Effects of terrain slope on water distribution and application uniformity for sprinkler irrigation. *Int. J. Agr. Biol. Eng.* **2018**, *11*, 120–125. [\[CrossRef\]](#)
- Hui, X.; Yan, H.; Zhang, L.; Chen, J. A simplified method to improve water distribution and application uniformity for sprinkler irrigation on sloping land: Adjustment of riser orientation. *Water Supply* **2021**, *21*, 2786–2798. [\[CrossRef\]](#)
- Zhang, L.; Fu, B.; Ren, N.; Huang, Y. Effect of pulsating pressure on water distribution and application uniformity for sprinkler irrigation on sloping land. *Water* **2019**, *11*, 913. [\[CrossRef\]](#)
- Yan, H.; Hui, X.; Li, M.; Xu, Y. Development in sprinkler irrigation technology in China. *Irrig. Drain.* **2020**, *69*, 75–87. [\[CrossRef\]](#)
- Silva, L.L. The effect of spray head sprinklers with different deflector plates on irrigation uniformity, runoff and sediment yield in a Mediterranean soil. *Agric. Water Manag.* **2006**, *85*, 243–252. [\[CrossRef\]](#)
- Chen, R.; Li, H.; Wang, J.; Song, Z. Critical factors influencing soil runoff and erosion in sprinkler irrigation: Water application rate and droplet kinetic energy. *Agric. Water Manag.* **2023**, *283*, 108299. [\[CrossRef\]](#)
- Lu, J.; Zheng, F.; Li, G.; Bian, F.; An, J. The effects of raindrop impact and runoff detachment on hillslope soil erosion and soil aggregate loss in the Mollisol region of Northeast China. *Soil Till. Res.* **2016**, *161*, 79–85. [\[CrossRef\]](#)
- Vaezi, A.R.; Ahmadi, M.; Cerdà, A. Contribution of raindrop impact to the change of soil physical properties and water erosion under semi-arid rainfalls. *Sci. Total Environ.* **2017**, *583*, 382–392. [\[CrossRef\]](#) [\[PubMed\]](#)
- Yan, H.J.; Bai, G.; He, J.Q.; Lin, G. Influence of droplet kinetic energy flux density from fixed spray-plate sprinklers on soil infiltration, runoff and sediment yield. *Biosyst. Eng.* **2011**, *110*, 213–221. [\[CrossRef\]](#)
- King, B.A.; Bjorneberg, D.L. Transient soil surface sealing and infiltration model for bare soil under droplet impact. *Trans. ASABE* **2012**, *55*, 937–945. [\[CrossRef\]](#)
- Al-Kayssi, A.W.; Mustafa, S.H. Modeling gypsiferous soil infiltration rate under different sprinkler application rates and successive irrigation events. *Agric. Water Manag.* **2016**, *163*, 66–74. [\[CrossRef\]](#)
- Hui, X.; Zheng, Y.; Meng, F.; Tan, H. Comprehensively evaluating and modelling droplet diameters and kinetic energies of low-pressure sprinklers. *Irrig. Drain.* **2022**, *71*, 829–854. [\[CrossRef\]](#)
- Huang, C.; Bradford, J.M.; Cushman, J.H. A numerical study of raindrop impact phenomena: The rigid case. *Soil Sci. Soc. Am. J.* **1982**, *46*, 14–19. [\[CrossRef\]](#)
- Chang, W.J.; Hills, D.J. Sprinkler droplet effects on infiltration. II: Laboratory study. *J. Irrig. Drain. Eng.* **1993**, *119*, 157–169. [\[CrossRef\]](#)
- Ghadir, H.; Payne, D. The formation and characteristics of splash following raindrop impact on soil. *Eur. J. Soil Sci.* **2010**, *39*, 563–575. [\[CrossRef\]](#)
- Chang, W.J.; Hills, D.J. Sprinkler droplet effects on infiltration. I: Impact simulation. *J. Irrig. Drain. Eng.* **1993**, *119*, 142–156. [\[CrossRef\]](#)
- Hui, X.; Yan, H.; Xu, Y.; Tan, H. Sprinkler droplet impact angle affects shear stress distribution on soil surface—a case study of a ball-driven sprinkler. *Water Supply* **2021**, *21*, 2772–2785. [\[CrossRef\]](#)
- Liu, J.P.; Yuan, S.Q.; Li, H.; Zhu, X.Y. Comparative research on hydraulic performance of sprinkler heads in sprinkler irrigation. In Proceedings of the ASABE International Meeting, Dallas, TX, USA, July 29–August 1 2012; American Society of Agricultural and Biological Engineers: St. Joseph, MI, USA, 2012; p. 1.
- Zhang, L.; Fu, B.; Hui, X.; Ren, N. Simplified method for estimating throw radius of rotating sprinklers on sloping land. *Irrig. Sci.* **2018**, *36*, 329–337. [\[CrossRef\]](#)
- Kruger, A.; Krajewski, W.F. Two-dimensional video disdrometer: A description. *J. Atmos. Ocean. Tech.* **2002**, *19*, 602–617. [\[CrossRef\]](#)
- Ge, M.; Wu, P.; Zhu, D.; Zhang, L. Analysis of kinetic energy distribution of big gun sprinkler applied to continuous moving hose-drawn traveler. *Agric. Water Manag.* **2018**, *201*, 118–132. [\[CrossRef\]](#)
- Huang, G.J.; Bringi, V.N.; Cifelli, R.; Hudak, D.; Petersen, W.A. A methodology to derive radar reflectivity–liquid equivalent snow rate relations using C-band radar and a 2D video disdrometer. *J. Atmos. Ocean. Tech.* **2010**, *27*, 637–651. [\[CrossRef\]](#)
- ISO 7749-2; Agricultural Irrigation Equipment-Rotating Sprinklers. 2: Uniformity of Distribution and Test Methods. ISO: Geneva, Switzerland, 2004.
- ISO 15886-3; Agricultural Irrigation Equipment-Sprinklers. 3: Characterization of Distribution and Test Methods. ISO: Geneva, Switzerland, 2012.

29. Hui, X.; Lin, X.; Zhao, Y.; Xue, M.; Zhuo, Y.; Guo, H.; Xu, Y.; Yan, H. Assessing water distribution characteristics of a variable-rate irrigation system. *Agric. Water Manag.* **2022**, *260*, 107276. [[CrossRef](#)]
30. Jiang, Y.; Liu, J.; Li, H.; Yong, Y. Droplet distribution characteristics of impact sprinklers with circular and noncircular nozzles: Effect of nozzle aspect ratios and equivalent diameters. *Biosyst. Eng.* **2021**, *212*, 200–214. [[CrossRef](#)]
31. Ghadiri, H.; Payne, D. The risk of leaving the soil surface unprotected against falling rain. *Soil Till. Res.* **1986**, *8*, 119–130. [[CrossRef](#)]
32. Hattori, S.; Kakuichi, M. Effect of impact angle on liquid droplet impingement erosion. *Wear.* **2013**, *298*, 1–7. [[CrossRef](#)]
33. Hui, X.; Zheng, Y.; Muhammad, R.S.; Tan, H.; Yan, H. Non-negligible factors in low-pressure sprinkler irrigation: Droplet impact angle and shear stress. *J. Arid Land.* **2022**, *14*, 1293–1316. [[CrossRef](#)]
34. DeBoer, D.W.; Monnens, M.J. Measurement of sprinkler droplet size. *Appl. Eng. Agric.* **2001**, *17*, 11–15. [[CrossRef](#)]
35. Zhang, L.; Hui, X.; Chen, J. Droplet diameter and kinetic energy intensity distribution regularities for sprinkler irrigation on sloping land. *Trans. CSAM* **2018**, *49*, 263–270. (In Chinese)
36. Hinkle, S.E. *Water Drop Ballistic with Drag Coefficient Dependent on Droplet Size and Velocity*; Paper No. 87-2596; American Society of Agricultural and Biological Engineers: St. Joseph, MI, USA, 1987.
37. Wobus, H.B.; Murray, F.W.; Koenig, L.R. Calculation of the terminal velocity of water drops. *J. Appl. Meteorol.* **1971**, *10*, 751–754. [[CrossRef](#)]
38. Hui, X.; Zhao, H.; Zhang, H.; Wang, W.; Wang, J.; Yan, H. Specific power or droplet shear stress: Which is the primary cause of soil erosion under low-pressure sprinklers? *Agric. Water Manag.* **2023**, *286*, 108376. [[CrossRef](#)]
39. Lehrsch, G.A.; Bjorneberg, D.L.; Sojka, R.E. Erosion: Irrigation-induced. In *Encyclopedia of Soils in the Environment*; Hillel, D., Ed.; Elsevier Ltd.: Oxford, UK, 2005; pp. 456–463.
40. Kincaid, D.C. The WEPP model for runoff and erosion prediction under sprinkler irrigation. *Trans. ASAE* **2002**, *45*, 67. [[CrossRef](#)]
41. Amiri, M.J.; Roohi, R.; Gil, A. Numerical simulation of Cd (II) removal by ostrich bone ash supported nanoscale zero-valent iron in a fixed-bed column system: Utilization of unsteady advection-dispersion-adsorption equation. *J. Water Process Eng.* **2018**, *25*, 1–14. [[CrossRef](#)]

Disclaimer/Publisher’s Note: The statements, opinions and data contained in all publications are solely those of the individual author(s) and contributor(s) and not of MDPI and/or the editor(s). MDPI and/or the editor(s) disclaim responsibility for any injury to people or property resulting from any ideas, methods, instructions or products referred to in the content.